Energy and Buildings 94 (2015) 177–188

Contents lists available at ScienceDirect

Energy and Buildings

journal homepage: www.elsevier.com/locate/enbuild

A combined cooling solution for high heat density data centers using multi-stage heat pipe loops

Hao Tian [a], Zhiguang He [b], Zhen Li [b,*]

[a] Institute of Optics, Fine Mechanics and Physics, Chinese Academy of Sciences, Changchun, 130033, China
[b] Key Laboratory of Thermal Science and Power Engineering of Ministry of Education, Department of Engineering Mechanics, Tsinghua University, Beijing, 100084, China

ARTICLE INFO

Article history:
Received 10 October 2014
Received in revised form 27 February 2015
Accepted 1 March 2015
Available online 9 March 2015

Keywords:
Data center
Distributed cooling
Multi stage
Heat pipe
Rack cooling

ABSTRACT

A combined cooling solution is proposed to improve both thermal and energy performance for data centers with high heat density. Multi-stage heat pipe is introduced to make the internally cooled rack, which helps to illuminate the undesired mixing of hot and cold air, and makes a uniform distribution of indoor temperature. A water loop of multi cold sources is designed to make full use of waterside free cooling potentials. With the switchable and flexible operating mode, an energy efficient cooling can be expected. An operating data center in Beijing is studied and retrofitted using this solution. A comparative measurement is performed to validate the effectiveness of this combined cooling solution, which shows an improved indoor thermal environment and reduces annual cooling cost by approximate 46%.

© 2015 Published by Elsevier B.V.

1. Introduction

With the fast development of IT industry, heat density in data centers increases rapidly, which imposes big challenges on heat removal. Data center is a specified enclosure accommodating devices for data processing and storage. In recent years, with the rapid growth of data processing performance, rack power has increased from less than 1 kW to more than 20 kW [1]. Normally, a data center with the average power density of more than 5 kW per rack can be classified as high heat density data center [2]. Such high heat density imposes big challenges on effective heat removal. As a result, the energy spent on thermal management has increased dramatically. Nowadays, the average annual cooling power consumption can reach as high as 30% of a data center's total operational cost [3]. Various solutions have been proposed to reduce cooling cost of high heat density data centers. However, due to the diversity of data center size, geometry, layout, power density and workload distribution, it is difficult to develop a feasible cooling solution that provides both efficient thermal and energy performance [4].

Currently, thermal management for most high heat density data centers uses air flow circulation to remove heat from racks to CRAC units. Cooling air is pumped into under floor plenum by CRAC units, and is distributed through perforated grid tiles under the floor, and is finally delivered to server racks. To manage airflow better, these perforated tiles are usually placed in front of the air-intake side of rack clusters, called cold aisles. After heat exchange, hot air exhausts into the space formed by the back side of rack clusters, called hot aisles. Hot air is pushed back to CRAC units through the upper space of data centers, or via special ducts or roof plenums. A typical airflow distribution in a high heat density data center is illustrated by Fig. 1.

The cold and hot aisle configuration is proposed to improve airflow performance and thermal management. However, such centralized terminals (CRAC units) sometimes cause undesired mixing of cool and hot air streams, such as when rack exhaust air flows into cold aisles, when cooling air flows back into CRAC units, and other forms of air leakage, which is illustrated by Fig. 2.

The airflow mal-distribution leads to a poor indoor thermal environment, especially non-uniform air temperatures and irregular humidity distribution in cold aisles. Such non-uniformity lowers the thermal reliability of data processing devices. To reduce this undesired air mixing, cold-aisle containment and blank space blocking are proposed and studied [5], illustrated by Fig. 3. It is

Abbreviations: CRAC, computer room air-conditioner; PUE, power utilization effectiveness; NTU, number of heat transfer unit; IT, information technology.

* Corresponding author at: Department of Engineering Mechanics, Tsinghua University, Beijing 100084, China. Tel.: +86 1062781610.
E-mail address: lizh@tsinghua.edu.cn (Z. Li).

http://dx.doi.org/10.1016/j.enbuild.2015.03.002
0378-7788/© 2015 Published by Elsevier B.V.

Nomenclature

Q	heat dissipation (W)
K	heat transfer coefficient (W/(m^2 K))
A	area (m^2)
c	specific heat (J/(kg K))
m	mass flow rate (kg/s)
η	overall effectiveness of heat transfer
t	temperature (°C)
ε	effectiveness of heat transfer for single heat exchanger
N	stage number
n	row number
V	velosity (m/s)
D	diameter (mm)
δ	thickness (mm)
d	distance (mm)

Subscripts and superscripts

in	inlet
out	outlet
w	water
f	refrigerant
f_{in}	fin
o	outer
t	tube
uw	upwind
h	heat transfer
r	row

supposed to completely isolate the cold air stream by sealing the entire cold aisle and all blank spaces among the racks.

However, airflow does not always follow the settled routes, leakage happens wherever possible, especially with large scale data centers. Referencing an operational raised floor cooling data center in Beijing, Fig. 4 provides air temperature and humidity distribution measurement for a cold aisle containment, with the average rack heat dissipation over 6 kW, and cooling air thermal conditions of 16.2 °C/71% inside the cold aisle. Large non-uniformity can be observed from the vertically measured air temperature and humidity along each rack. Similar phenomena can be observed for other physical isolation oriented design, such as overhead returns with ceiling vents or ducts and their combination [5].

To meet the minimum thermal requirements for servers located at the worst positions inside the cold-aisle containment (near the top of racks in Fig. 4), colder chilled water or larger air flow rate is commonly seen as state-of-the-art at the price of higher energy penalty. Since indoor air flow has significant impact on both

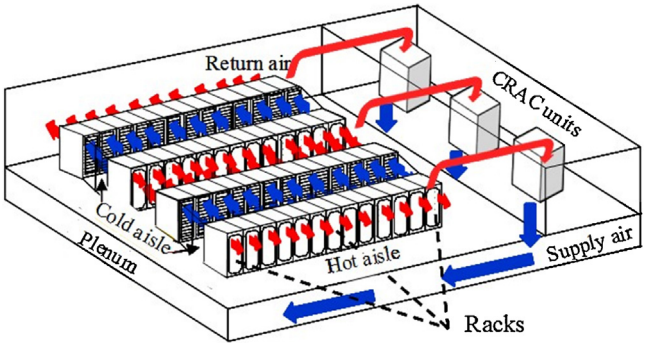

Fig. 1. Typical data center airflow with cold/hot aisle layout.

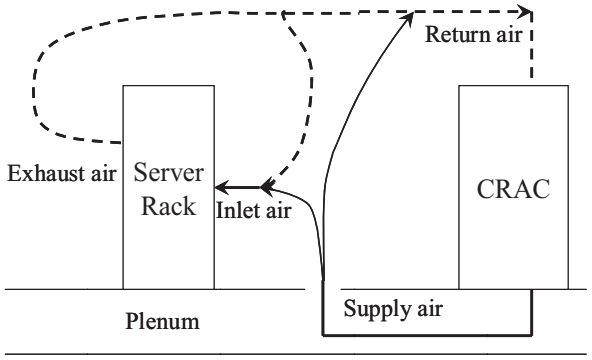

Fig. 2. Undesired air mixing.

thermal and energy performance of data center cooling, a literature review should be performed before any new solution is proposed.

Nowadays, there are three major research areas focused on improving data center airside performance, covering the design, simulation and optimization of data center.

Most research on data center design relies on engineering experience, field measurements and mathematical correlation. Sharma et al. [6] proposed a thermal effectiveness based evaluation for data center layout. Rambo and Joshi [7] characterized the overall efficiency of data centers based on minimum temperature and entropy gradient principle. They considered the air flow performance from under floor plenum to perforated tiles as a significant influence factor. Kang et al. [8] used a simplified correlation to describe the air movement and evaluate air flow performance through perforated tiles of different forms and arrangement, with the assumption of uniform plenum pressure. Recently, official guidelines for data center operation, including recommended layout, thermal environment and management, have been published by the American Society of Heating, Refrigeration, and Air-conditioning Engineers (ASHRAE) [9]. These technical standards [9,10] are raised with each new research findings and technology advancement.

Simulation is another important approach to study data center thermal behavior with low cost. CFD (Computational Fluid Dynamics) software helps to better understand the underlying physical characteristics of heat transfer in data center space by numerically computing the air flow and convective heat exchange. As computer science develops rapidly, numerical simulation is proving to play an

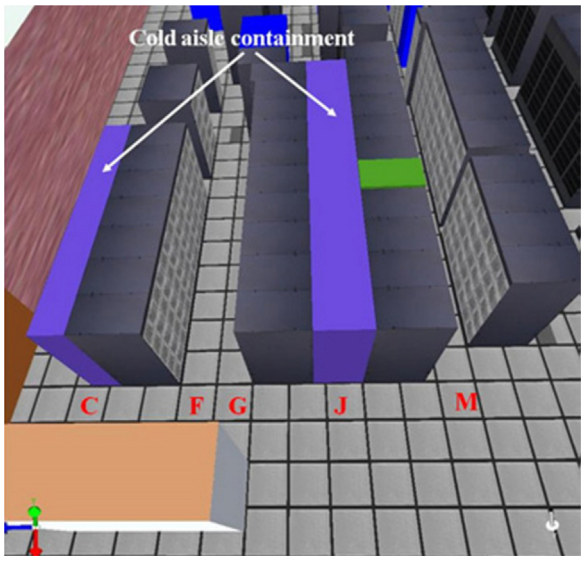

Fig. 3. Schematic of cold-aisle containment in data centers.

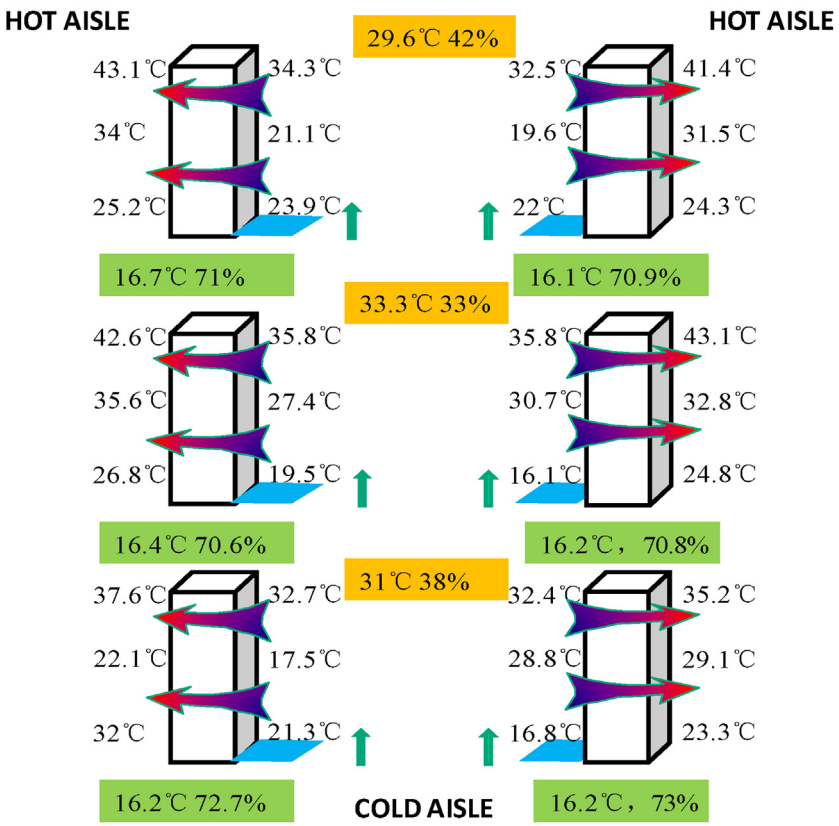

Fig. 4. Measurement of air temperature/humidity distribution in the cold-aisle containment.

irreplaceable role in data center thermal analysis. Patel et al. [11,12] computed the steady state temperature profile and air movement for a raised floor data center using rack intake air temperature as the evaluating metric for several typical rack layouts. Rambo and Joshi [13,14] studied characteristics of turbulence air flow in data centers using RANS model, and performed detailed thermal simulation inside racks. Shrivastava et al. [15] used a multi-scale CFD model to evaluate the cooling effectiveness of data centers with under floor plenum and roof diffusers. Iyengar et al. [16] performed a similar study without under floor plenum, to compare rack intake air temperature by changing rack layout and diffuser position. The rack intake air temperature once again is considered as the feasible metric to assess room level thermal. Schmidt and Cruz [17] studied air behavior through different types of perforated tiles and the impact on data center temperature distribution by simulation and measurement. Radmehr et al. [18] analyzed the influence of air leakage around perforated tiles, including reverse flow and short circuits, on data center thermal environment. In addition, a CFD based prediction on air flow performance is validated and correlated by measurements. Rambo and Joshi [19] made a detailed 2D simulation and correlation on air flow rate and distance between CRAC units and perforated tile line. Van Gilder and Schmidt [20] studied the impact of under floor plenum depth and tie open area proportion on air flow uniformity through perforated tiles using a raised floor data center CFD model. Such effect is compared for several data center layouts by simulation.

Optimization is an overall redesign based on investigation, measurement and analysis. New strategies and solutions of energy efficient cooling for high heat density data centers have emerged recently [21–40]. With the introduction or combination with technologies like heat pipe air-conditioner [31,34,36,37], solar cooling [30], evaporative cooling [32], cold storage [39,40] and other integrated cooling modes [38], chiller operating time or chiller load is reduced, and more free cooling becomes available. Facebook's new built data center located at Prinevill in Oregon removes all heat dissipated by servers using natural ventilation only, profiting from the local climate. This full free cooling solution earns remarkable energy benefits for data center thermal management, with an annual PUE value as low as 1.073, indicating that 93% of data center annual energy consumption flows into data processing equipment [41]. IBM's data center uses waste heat for space heating and natural ventilation for indoor humidity control. Combined with specially designed micro-channel liquid coolers for blade server cooling, the annual power consumption for data center thermal management is reduced by about 40% on average [42,43]. Google's data center uses evaporative cooling to reduce chiller operating time [44]. Thermacore's so called Therma-Bus Tech proposes an effective liquid cooling solution for high performance chips such as multi-core CPUs and high speed microprocessors, using output water loop of cooling towers to remove heat directly from data processing devices to the outdoor environment [45].

All the work above have proposed new methods and solutions based on theoretical, technical and operational innovation, which greatly improved the development of thermal management for high heat density data centers.

2. Multi-stage heat pipe loop

As illustrated by Fig. 5, with the cooling terminals located inside the rack, the entire heat exchange of the air flow loop is sealed inside, and physically isolated from other racks. Such cooling terminal has been used and studied recently [46]. However, there is an inevitable risk of water leakage for such water-cooling terminals, which is extremely dangerous to data processing devices. A safety-adaptive rectification to the rack-cooling terminal is necessary.

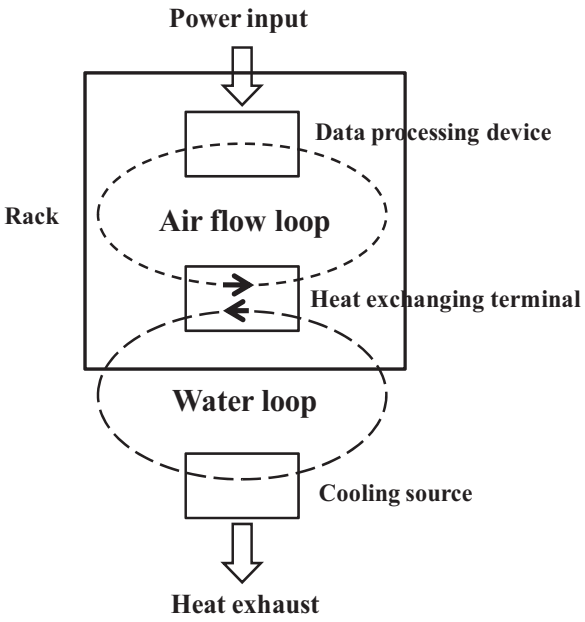

Fig. 5. Schematic of distributed cooling solution.

Because of the non-detrimental leakage and good heat conduct performance, the R22 is selected as suitable two-phase heat exchanging fluid to efficiently transport heat from the terminals to the cold sources, with detailed design illustrated in Section 3. For a given data center with fixed heat dissipation and heat exchanger input, a smaller temperature difference between air flow loop and water loop means less dissipation of heat transport potential [31]. In other words, a better performance of heat exchanging terminals in Fig. 5 means a higher cold source temperature, which means more potential for waterside free cooling. Therefore, how to reduce the temperature difference spent on the heat pipe heat exchanger becomes a key issue.

Effectiveness of heat transfer (defined by Eq. (2) and (3) [47]) is used to evaluate the thermal performance of water (counter flow) and heat pipe media heat exchangers (illustrated by Fig. 6).

$$\mathrm{NTU} = \frac{KA}{cm} \tag{1}$$

$$\eta_{\mathrm{heat-pipe}} = 1 - \mathrm{e}^{-\mathrm{NTU}} \tag{2}$$

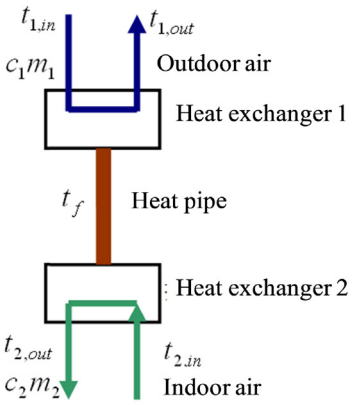

Heat pipe media heat exchanger

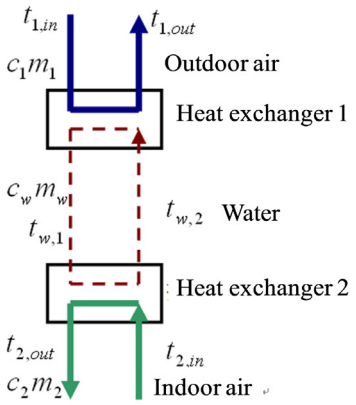

Water media heat exchanger

Fig. 6. Indirect heat exchanger using heat pipe/water as media.

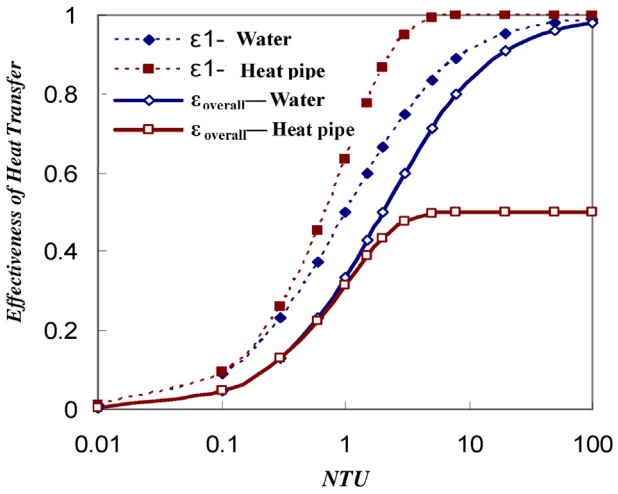

Fig. 7. Performance comparison of the two heat exchangers (Logarithmic Coordinates).

$$\eta_{\mathrm{water-air}} = \frac{1 - \exp\left\{(-\mathrm{NTU})\left[1 - \frac{(cm)\min}{(cm)\max}\right]\right\}}{1 - \frac{(cm)\min}{(cm)\max}\exp\left\{(-\mathrm{NTU})\left[1 - \frac{(cm)\min}{(cm)\max}\right]\right\}} \tag{3}$$

Table 1 lists the calculations of heat transfer effectiveness using NTU with uniform mass flow rate distribution. For detailed deduction, view Refs. [48–50].

Fig. 7 compares the effectiveness of heat transfer between water and heat pipe heat exchanger. It can be seen from Fig. 7 that in condition of infinite *KA*, the water media heat exchanger has the highest overall effectiveness of 1, while that of the single-heat pipe media is only 0.5, indicating a large potential for the optimization of heat pipe arrangement.

In order to further improve the overall effectiveness of heat pipe media heat exchangers, a multi-stage connection is proposed, illustrated by Fig. 8. Compared with the single stage heat pipe, multi media temperature t_{fi} is more similar to water media temperature.

Assuming an *N*-stage heat pipe media heat exchanger with uniform NTU and air flow rate *cm* of outdoor and indoor unit in each stage. According to Table 1, the overall effectiveness of heat transfer for each stage and the entire system can be calculated by Eqs. (4) and (5).

$$\eta 1 = \eta 2 = \cdots \eta N = \frac{\varepsilon}{2} = \frac{1}{2}\left(1 - \mathrm{e}^{-\frac{\mathrm{NTU}}{N}}\right) \tag{4}$$

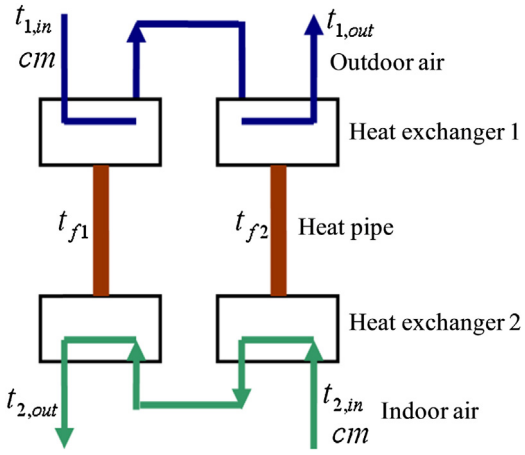

Fig. 8. Two-stage heat pipe media heat exchanger.

$$\eta = \frac{N\eta N}{1+(N-1)\eta N} = \frac{\frac{N}{2}\left(1-e^{-\frac{NTU}{N}}\right)}{1+\frac{1}{2}(N-1)\left(1-e^{-\frac{NTU}{N}}\right)} \tag{5}$$

Some important conclusions can be deduced from Eq. (5).

Given stage number N and infinite NTU, the overall effectiveness of each stage heat pipe media heat exchanger is 0.5, and the overall effectiveness of the entire system can be calculated by Eq. (6).

$$\eta = \frac{N}{N+1} \tag{6}$$

Given NTU and infinite stage number N, the overall heat transfer effectiveness of the entire system will be the same as water media heat exchanger, calculated by Eq. (7).

$$\eta = \frac{\mathrm{NTU}}{\mathrm{NTU}+2} \tag{7}$$

Given infinite NTU and infinite stage number N, the overall heat transfer effectiveness of the entire system will be 1.

Fig. 9 illustrates the variation of the overall heat transfer effectiveness with NTU values for water and multi-stage (stage number N from 1 to 30) heat pipe media heat exchangers.

It can be seen from Fig. 9 that, compared with the single stage heat pipe, multi-stage heat pipe heat exchanger shows better thermal performance, which enables smaller temperature difference between air loop and water loop.

Fig. 9 also shows that with fixed NTU, the overall effectiveness of multi-stage heat pipe heat exchanger increases with stage number N. When N keeps increasing, the thermal performance of multi-stage heat pipe comes closer to that of water media heat exchanger, especially within the commonly used NTU values (0.5–2). However, the complexity and initial cost also increase with stage number N.A two-stage heat pipe heat exchanger is finally chosen for the balance of thermal performance and engineering feasibility.

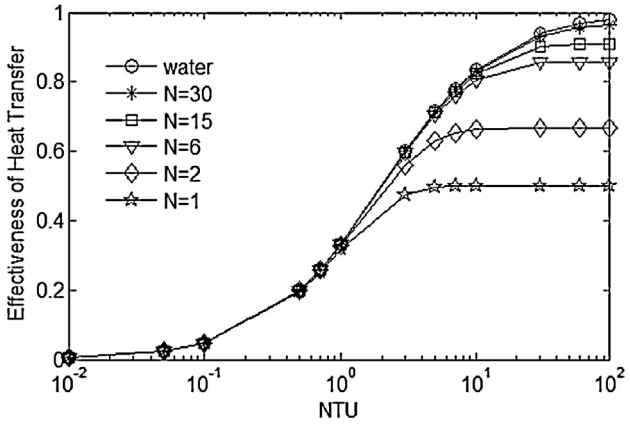

Fig. 9. Performance comparison of the two heat exchangers (Logarithmic Coordinates).

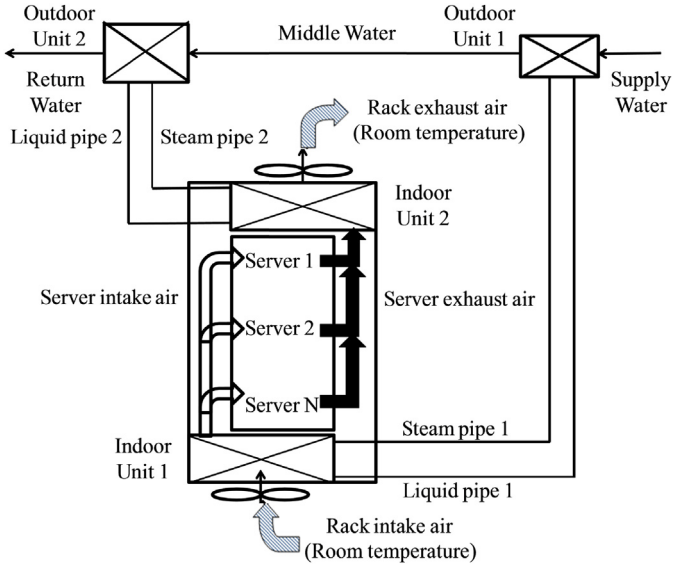

Fig. 10. Schematic of the internally cooled rack.

3. Distributed cooling terminal

An internally cooled rack is proposed as distributed cooling terminal using two-stage heat pipe media heat exchangers illustrated by Fig. 10.

The two heat pipe loops, illustrated by Fig. 11, each consists of two heat exchange units (indoor/outdoor unit) and two fluid pipes (liquid/steam pipe), connects the air flow loop and cooling water loop in series. The indoor unit 1 is installed at the bottom of the rack to cool the rack intake air from indoor temperature (23–25 °C) to server required intake temperature (18–20 °C) by supply water (10–12 °C). While indoor unit 2 is installed at the top of the rack to cool the server exhaust air (35–40 °C) to indoor temperature (23–25 °C) by the output water of outdoor unit 1 (13–15 °C). The

Table 1
Calculation of effectiveness of heat transfer.

	Heat pipe media heat exchanger ($c_1m_1 = c_2m_2$)	Water media heat exchanger ($c_1m_1 = c_2m_2 = c_wm_w$)
Effectiveness of Heat Exchanger 1	$\varepsilon_1 = \frac{t_{1,in}-t_{1,out}}{t_{1,in}-t_f} = 1-e^{-NTU_1}$, $NTU_1 = \frac{K_1A_1}{c_1m_1}$	$\varepsilon_1 = \frac{t_{1,in}-t_{1,out}}{t_{1,in}-t_{w,2}} = \frac{NTU_1}{1+NTU_1}$, $NTU_1 = \frac{K_1A_1}{c_1m_1}$
Effectiveness of Heat Exchanger 2	$\varepsilon_2 = \frac{t_{2,out}-t_{2,in}}{t_f-t_{2,in}} = 1-e^{-NTU2}$, $NTU_2 = \frac{K_2A_2}{c_2m_2}$	$\varepsilon_2 = \frac{t_{2,out}-t_{2,in}}{t_{w,1}-t_{2,in}} = \frac{NTU_2}{1+NTU_2}$, $NTU_2 = \frac{K_2A_2}{c_2m_2}$
Overall Effectiveness	$\eta = \frac{t_{2,out}-t_{2,in}}{t_{1,in}-t_{2,in}} = \frac{\varepsilon_1\cdot\varepsilon_2}{\varepsilon_1+\varepsilon_2}$	$\eta = \frac{t_{2,out}-t_{2,in}}{t_{1,in}-t_{2,in}} = \frac{1}{\frac{1}{\varepsilon_1}+\frac{1}{\varepsilon_2}-1}$
Overall Effectiveness ($K_1A_1 = K_2A_2$)	$\eta = \frac{\varepsilon_1}{2} = \frac{1}{2}\left(1-e^{-NTU}\right)$	$\eta = \frac{\varepsilon_1}{2-\varepsilon_1} = \frac{NTU}{NTU+2}$

Table 2
Chiller performance comparison.

Operating mode	Component	Evaporator NTU	Inlet/output temperature (°C)	Evaporation temperature (°C)	Condensation temperature (°C)	COP
Single-chiller	Chiller	2	14/10	9.2	45	2.75
Multi-chiller	Chiller 2	2	18/14	13.4	45	2.98
	Chiller 1	2	14/10	9.4	45	

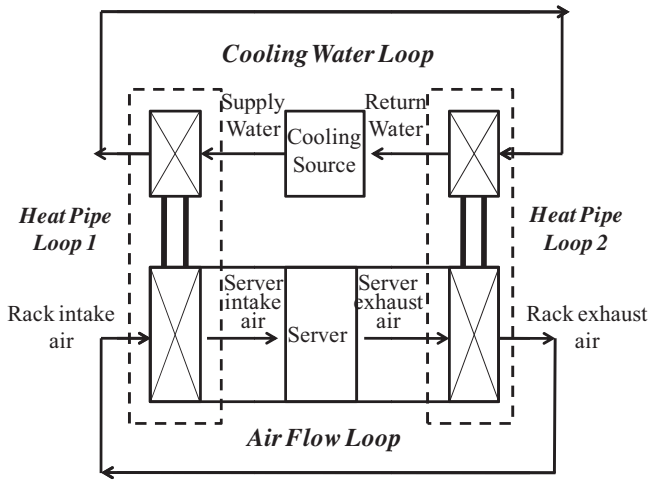

Fig. 11. Schematic of heat pipe loops.

output water of outdoor unit 2 (return water, 22–24 °C) is cooled by the cold source and finally delivers all heat to outdoor environment.

Air intake temperature is set by Class A1 Grade recommended by ASHRAE guidelines [10], in which the environmental grade for different types of IT equipment in data center is shown by Fig. 12.

In order to fit the server load variation and maintain a uniform intake/exhaust air temperature, the amount of heat exchanged by each unit in the heat pipe loops can be adjusted through fan speed control. Such configuration achieves uniform indoor air temperature distribution and the cold and hot aisle can be replaced by more racks. For indoor humidity control, a few dehumidifiers are arranged at each corner of the room to maintain a recommended rack intake air relative humidity of 35–50%[10].

4. Combined water loop

To further improve outdoor free cooling potential and energy performance, a combined water loop with multi-cold source is designed to provide large temperature difference between supply and return water (~10°C), meeting the requirement of temperature-matched heat transfer [51], illustrated by Fig. 13. Two chillers and one open cooling tower are connected in series as switchable cold source, which provide cooling water of required temperature. With two heat pipe outdoor units and one pump integrated, the water loop transfers the heat from heat pipe loops to outdoor environment.

The multi-cold source enables the water loop to automatically distribute cooling load and choose cold source, according to the availability of waterside free cooling. With fixed supply/return water temperature (10–12 °C/22–24 °C), the operating mode of the multi-cold source is decided by the output water temperature of the cooling tower, which is mainly determined by outdoor air wet bulb temperature [52]. When outdoor wet bulb temperature is low enough, all cooling load is undertaken by the cooling tower. When that temperature is not sufficiently low, chillers and the cooling tower co-work to share the cooling load, with chillers started one by one. When that temperature is too high to use the cooling tower, all heat is removed by chillers.

To quantify the performance advantage of multi-chiller arrangement and find the optimum cooling load distribution among the co-operating chillers, the chiller's COP is analyzed and compared with the single-chiller mode under following conditions:

(1) The same total cooling load.
(2) The same outdoor conditions.
(3) The same total evaporator area.
(4) The same condensation temperature.

Detailed information is shown in Table 2.

It is noted that compared to the single-chiller mode, each chiller of the multi-chiller mode shares half evaporator area and half water flow rate, according to Eq. (1), it is reasonable to assume a uniform evaporator NTU value for each chiller in each mode.

The comparison shows a higher COP of a multi-chiller mode than that of a single-chiller mode. If the lower pump power consumption is considered, a better energy performance for the combined water

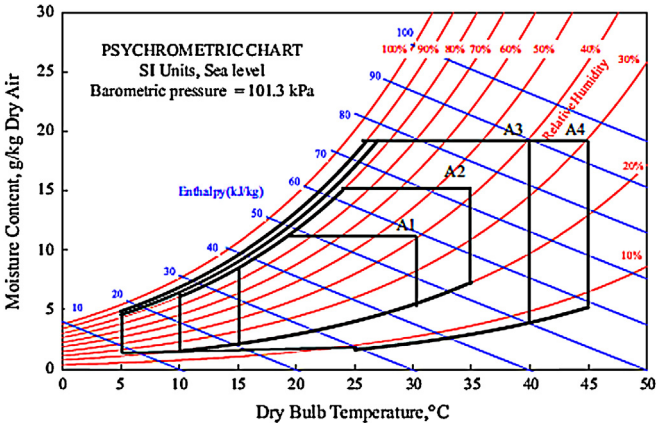

Fig. 12. ASHARE environmental classes for data centers.

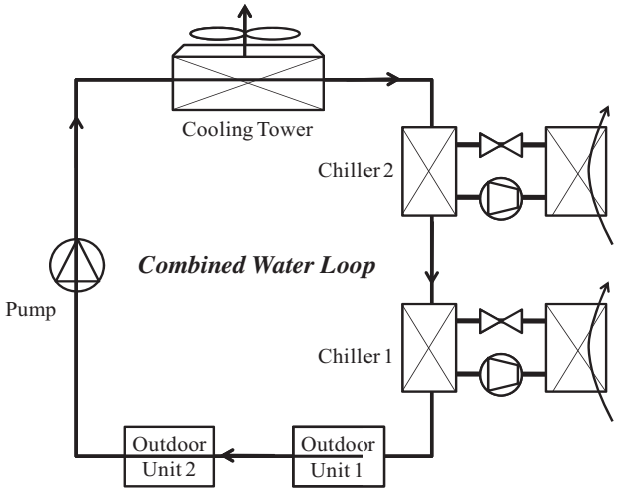

Fig. 13. Schematic of the combined water loop.

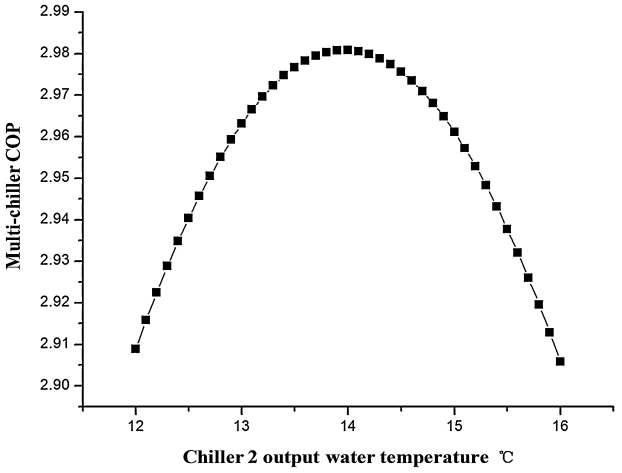

Fig. 14. Multi-chiller COP curve.

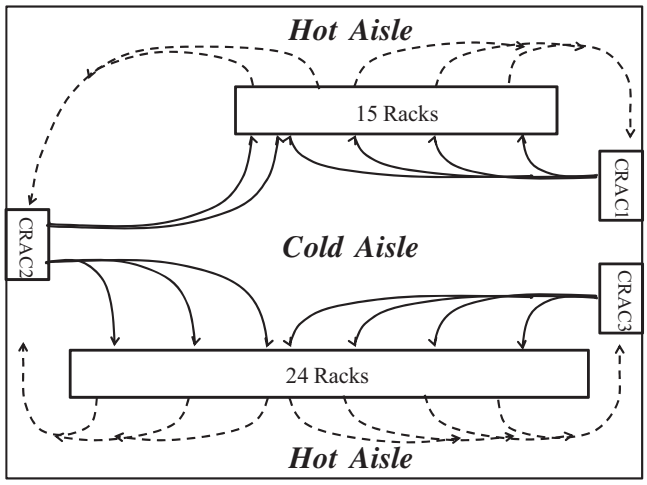

Fig. 15. Data center layout and air flow.

loop can be expected through the co-operating of two chillers. It also can be seen that with other conditions fixed, the COP of multi-chiller is decided by the cooling load distribution, or the output water temperature of chiller 2. The COP curve is shown by Fig. 14, based on Table 2, indicating the optimum operating performance in condition of uniform cooling load distribution for each chiller. This conclusion is useful to optimize the co-operating conditions.

According to the statistical outdoor weather data of Beijing, assuming the wet bulb efficiency of the cooling tower to be 75%[30], and supply/return temperature of the combined water loop to be 10/20 °C, Table 3 shows the calculation of the theoretical annual operating time of each chiller and cooling tower in Beijing. It must be noted that the calculation is based on certain ideal assumption and simplification, which may be quite different from the actual working conditions. Therefore, the results can only be used for reference.

It can be seen that for the combined water loop, the annual percentage of chiller total operating time is less than 50%, with annual full load operating time percentage less than 20%. Meanwhile, the annual percentage of cooling tower total operating time is more than 80%, with annual full load operating time percentage more than 40%. Such operating mode enables the cooling tower to undertake as more cooling load as possible, and decreases the full load operating time of chillers. Therefore, the energy cost of the water loop can be reduced.

5. Case study

An operating data center in Beijing is retrofitted using distributed terminals and the combined water loop. To verify the effectiveness of this cooling solution, a measurement based comparison on both thermal and energy performance of the two cooling systems is performed, in condition of similar cooling load and outdoor conditions.

Table 3
Operating mode of the combined water loop in Beijing.

Outdoor air wet bulb temperature	Cooling tower operating hours	Chiller2 operating hours	Chiller1 operating hours
≤6°C	3848	0	0
6–13°C	1458	1458	0
13–19°C	1721	1721	1721
>19°C	0	1733	1733
Partial load	3179	3179	1721
Full load	3848	1733	1733
Total	7027	4912	3454

The basic information of the data center before retrofitting is shown in Table 4.

Fig. 15 illustrates the data center layout and air flow before retrofitting. The data center uses non-raised floor or ceiling return layout with cold and hot aisles. The cooling air (solid lines) is delivered to the cold aisle by three CRAC units, with hot air (dashed lines) sent back through upper and lateral space.

5.1. Performance measurement (before retrofitting)

Indoor air temperature distribution is measured to evaluate the air flow performance. Fig. 16 shows the time averaged temperature distribution of rack intake air at several typical locations during January 15th, 2011, with the measurement error due to the reliability of metering methods, accuracy of metering devices and other influence factors controlled within ±0.5 °C, and the temperature data is collected every ten minutes. The measurement shows a quite non-uniform distribution. There are 27 racks with intake air temperature over 25 °C while only two racks below 15 °C, in condition of the CRAC supplied air temperature of 12 °C. Such non-uniform distribution indicates a poor indoor air flow performance with a massive undesired air mixing.

Real-time measurement of return air temperature for each CRAC unit during January 15th, 2011 is illustrated by Fig. 17, with the measurement error controlled within ±0.5 °C and data collected every ten minutes. The maximum return air temperature difference can be 6 °C. The non-uniformity of return air temperature can lead to an unfavorable cooling load distribution among the CRAC units and finally will affect the COP detrimentally.

Fig. 18 demonstrates the real-time measurement of CRAC's COP during January 15th, 2011, The cooling load of CRAC units is

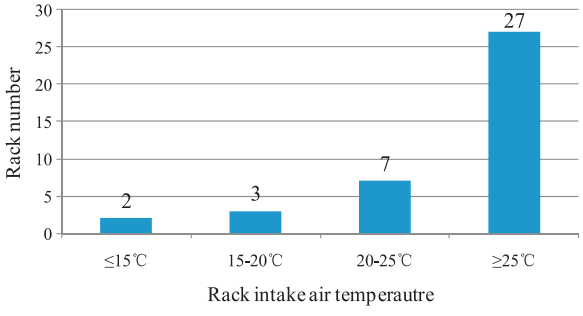

Fig. 16. Temperature distribution of rack intake air.

Table 4
Basic information of the data center in Beijing.

Data center size 18 m × 5.5 m × 3 m	External wall 1	Rack number 39	Total rack power 50–60 kW
CRAC unit number 3	CRAC cooling capacity80 kW	Indoor temperature 20–28 °C	Indoor humidity 40–70%

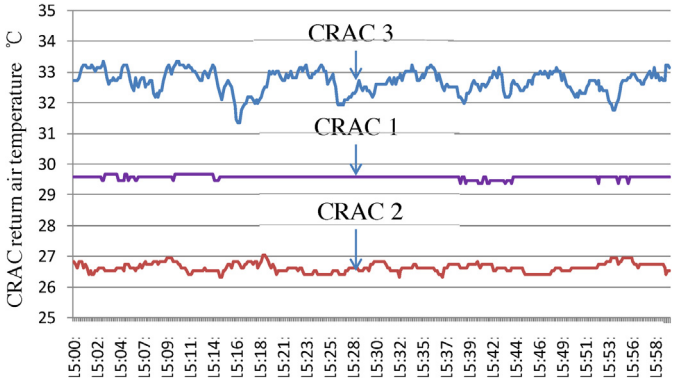

Fig. 17. Real-time return air temperature measurement.

approximately equalized by the power consumption of all servers, due to the ignorable heat transported through the external walls, shown by Fig. 19. All power data is measured by real-time power metering devices, with the measurement error controlled within ±0.5 kWand data collected every ten minutes.

Fig. 20 shows the measurement of the real-time outdoor dry bulb temperature during the same day, with the measurement error controlled within ±0.5°C and data collected every 10 min. The announced COP by the CRAC manufacturer is 3.5–4.0 under the similar cooling load and outdoor condition. The measurement shows an unsatisfied energy performance of the CRAC units.

Fig. 21 shows the daily-averaged intake and exhaust air temperature of all racks in January, 2011, with the measurement error controlled within ±0.5°C. As we can see, the difference between intake air temperature and exhaust air temperature is as large as 7.5 °C averagely.

The measurement on both the indoor air flow performance and CRAC energy performance shows a practical demand for the retrofitting of cooling system.

5.2. *Performance measurement (after retrofitting)*

The combined water loop using distributed cooling terminals proposes a feasible solution for the retrofitting demand. Fig. 22 shows the photos of the internally cooled racks filled with operating servers, using specially designed two-stage heat pipe loops.

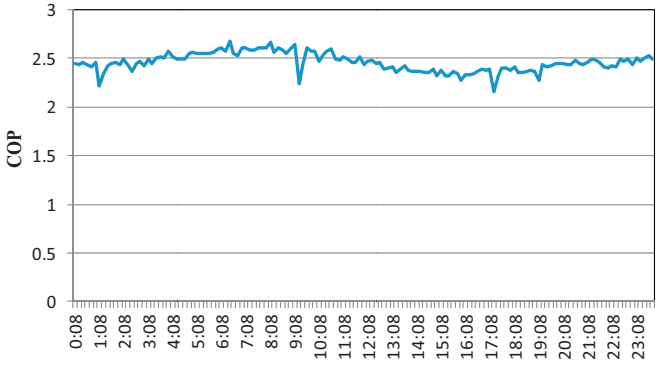

Fig. 18. Real-time COP of CRAC units on January 15th.

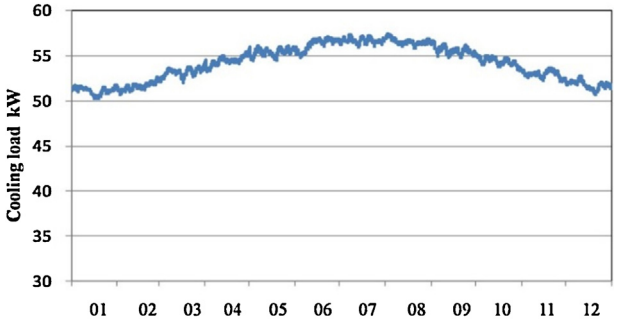

Fig. 19. Annual cooling load of the data center (Calculated by DeST).

Figs. 23 and 24 shows the measurement of the daily-averaged air temperature and humidity distribution inside one rack in June, 2012, with the measurement error controlled within ±0.5 °C and ±5%, respectively. The measurement shows that, for that rack, the curve of intake air almost coincides with that of exhaust air, basically the same as indoor temperature (23–25°C). And the server intake air temperature of that rack varies from 17.4 to 22°C, with the relative humidity changing from 39% to 64%, both fit the guidelines recommended by ASHRAE [10].

The measurement of the daily-averaged intake and exhaust air temperature and humidity of all 39 racks in June 6th, 2012 is demonstrated by Figs. 25 and 26, with the measurement error controlled within ±0.5 °C and ±5%. It can be seen that, after retrofitting, the largest temperature difference between the intake and exhaust air for a single rack is less than 3.5 °C, with the averaged value of 1.4 °C for all 39 racks. The maximum humidity difference for one single rack is 10%, with the averaged value of 5% for all 39 racks.

It also can be seen that, during that day, the indoor air temperature changes from 20 to 26 °C, and the humidity varies from 30% to 60%, basically in accordance with the measured values shown by Figs. 23 and 24.

The daily averaged intake and exhaust air temperature of all racks in January, 2012 is showed in Fig. 27, with the measurement error controlled within ±0.5 °C. It can be seen that, compared with Fig. 21, which shows the measurement before retrofitting in the same month, 2011, the largest temperature difference between the intake and exhaust air is less than 2.5 °C, which shows a better indoor cooling.

The indoor measurement above shows that compared with the air temperature and humidity distribution before retrofitting, the internally cooled racks create a more uniform indoor temperature

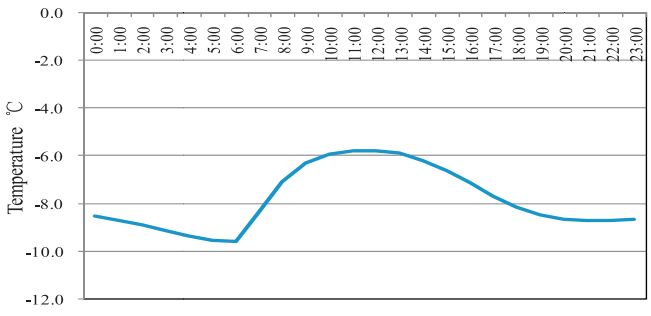

Fig. 20. Real-time outdoor dry bulb temperature on January 15th.

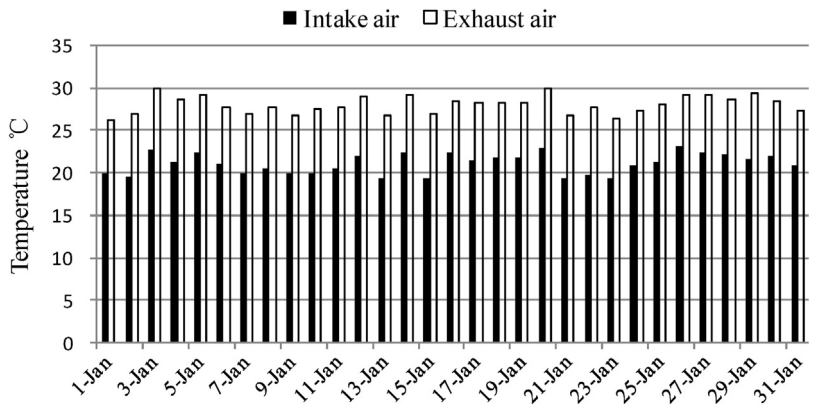

Fig. 21. Daily-averaged intake and exhaust air temperature of all racks in January, 2011.

Fig. 22. Internally cooled racks using two-stage heat pipe loops.

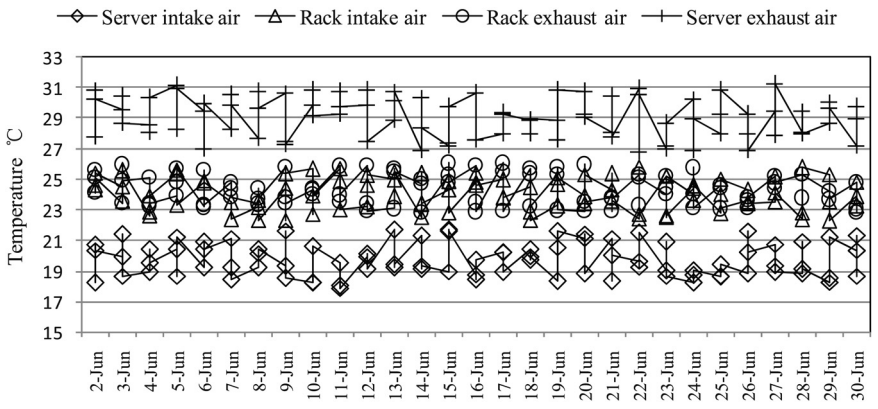

Fig. 23. Daily-averaged air temperature inside the chosen internally cooled rack in June.

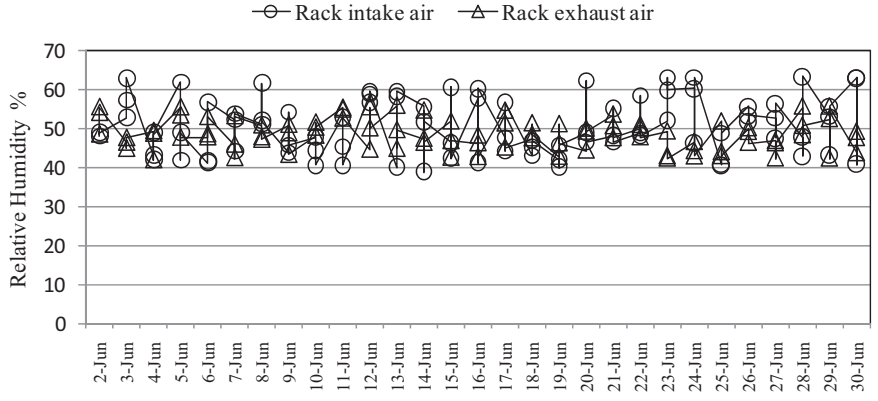

Fig. 24. Daily-averaged air humidity inside the chosen internally cooled rack in June.

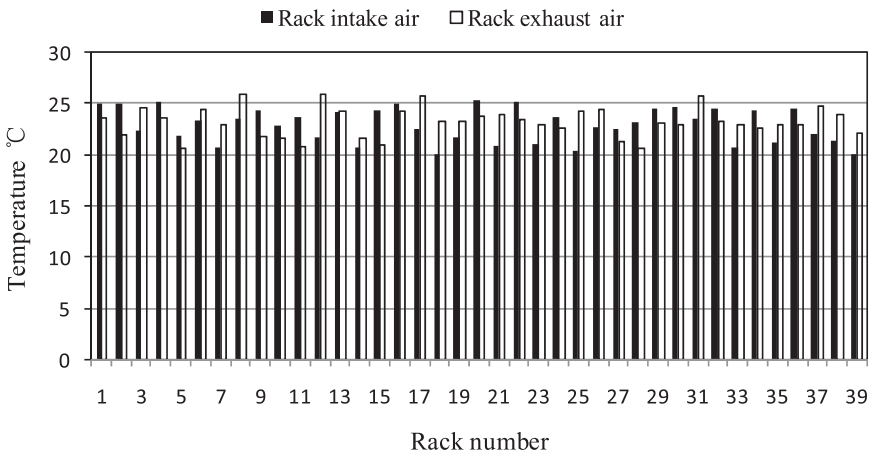

Fig. 25. Daily-averaged intake and exhaust air temperature of all racks in June 6th.

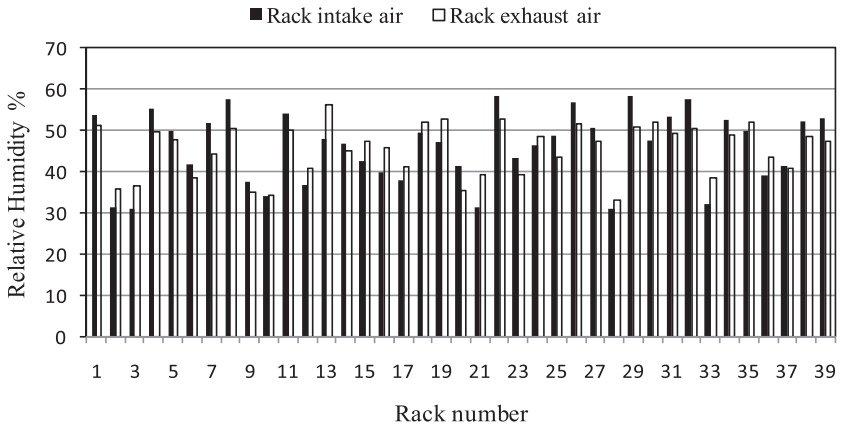

Fig. 26. Daily-averaged intake and exhaust air humidity of all racks in June 6th.

and humidity by effectively reducing the cold and hot air mixing. The distributed cooling terminals improve the air flow performance and show a good agreement with the initial design.

The daily-averaged temperature distribution of the combined water loop during June, 2012 is illustrated by Fig. 28, with the measurement error controlled within ±0.5 °C and data collected every hour. The measurement shows a uniform cooling load allocation for each heat pipe loop, which is in accordance with the air temperature distribution inside the rack measured by Fig. 23, and fits the initial design well.

Chiller performance is measured and compared between the single-chiller and multi-chiller operating mode during June, 2012. The COP curve is illustrated by Fig. 29, with the temperature/power measurement error controlled within ±0.5°C/±0.5 kW and data collected every half an hour. The measurement shows a better energy performance of co-operating chillers, which agrees with the analysis in Table 2.

Table 5 validates the performance of the combined water loop, through the comparison of the measured and designed conditions (workload, operating time) for each major component after

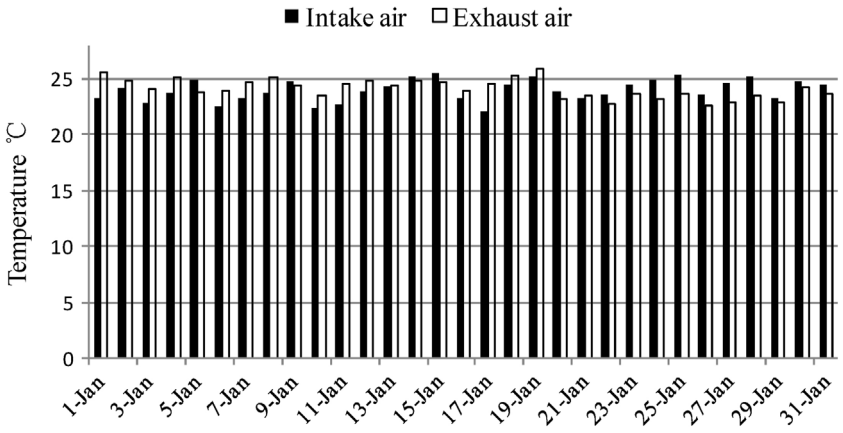

Fig. 27. Daily-averaged intake and exhaust air temperature of all racks in January, 2012.

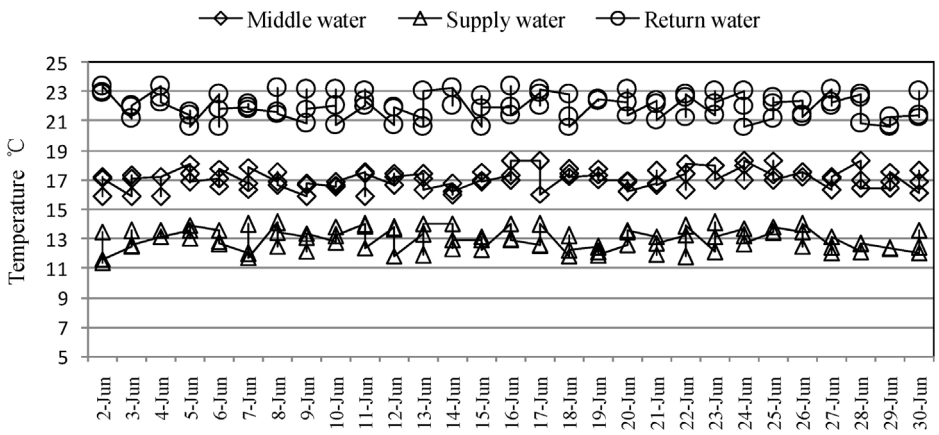

Fig. 28. Daily-averaged water temperature distribution in June, 2012.

Table 5
Performance validation.

Performance	Full load operation hours		Partial load operation hours		Total operation hours	
Data type	Design	Measurement	Design	Measurement	Design	Measurement
Cooling tower	3848	3550	3179	2877	7027	6427
Chiller 2	1733	2175	3179	3400	4912	5575
Chiller 1	1733	2069	1721	2215	3454	4284

a whole year operation, with the measurement error controlled within ±10%. The measurement shows an acceptable agreement with the design.

Table 6 compares the annual operating performance between the two cooling systems, using two energy-related indexes, energy efficiency ratio (EER, defined by Eq. (8) [30]) and the energy usage effectiveness (PUE, defined by Eq. (9) [1]).

$$\mathrm{EER} = \frac{W}{Q} \tag{8}$$

$$\mathrm{PUE} = \frac{P}{P'} \tag{9}$$

In which, W stands for the total power consumption of all cooling components, Q represents total cooling load. P stands for the total power consumption of the data center, P' represents the power consumed by all data processing devices. All power consumption data is acquired through the real-time power metering devices.

During the whole year 2011 which is before retrofitting and 2012 which is after retrofitting, the server workload distribution basically remained the same, with no other interruptions (such as massive or long time renewal, updating or maintenance of servers). The measurement error due to the reliability of metering methods, accuracy of metering devices and other influence factors is controlled within ±20%.

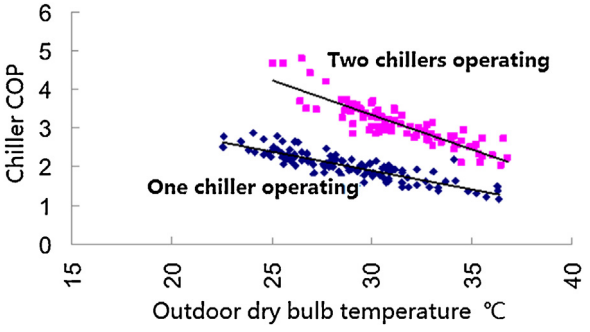

Fig. 29. Chiller performance measurement.

Table 6
Annual operating performance comparison.

	Averaged PUE	Averaged EER
Before retrofitting	1.39	2.6
After retrofitting	1.21	4.8

It can be seen from Table 6 that, compared to former CRAC system, the combined cooling solution effectively reduced the annual cooling energy consumption by about 46%. And total annual energy cost by the entire data center has been reduced by about 13%.

The total retrofitting cost is 350000 CNY, 3500 CNY per square averagely, and this price reduces with the increase of data center area and installed capacity. The annual average power consumption of CRAC system before and after retrofitting is 185,000 and 100,000 kWh, respectively. Approximately 46% of the cooling cost is saved per year after retrofitting. According to the general industrial electricity price 0.8 CHY per kWh, it will save 68000 CHY every year, and the pay back period is about 4 years.

6. Conclusions

Aimed at better energy and thermal performance, a distributed cooling solution is proposed for high heat density data centers. Based on the least dissipation theory and property matched heat exchange principle, the internally cooled rack with two-stage heat pipe loops and a combined water loop with serially connected multi cold sources is designed, which can dynamically and effectively adjust the cooling load distribution according to the variation of both server workloads and outdoor conditions. Such method uses specific rack to improve airside performance, which allows flexible application to scalable data centers. The versatility of waterside efficient cooling is guaranteed by the common water loop, which has switchable operating mode between chiller and free cooling according to different outdoor conditions.

The measurement based on study of a retrofitted data center validates the performance of the distributed cooling system. The measurement shows that, compared with the former CRAC system, the new cooling solution effectively improves the thermal

reliability of data processing devices and reduces cooling energy cost by about 46%. The internally cooled racks improve indoor air flow performance, basically eliminate undesired air mixing and hot spots, and create a more uniform indoor thermal environment. In addition, the distributed cooling solution cancels the cold and hot aisle layout and increases the indoor space utilization. The combined water loop shows better energy performance, with annual cooling power consumption reduced by about 13%.

This study provides a feasible cooling solution for high heat density data centers, future work may focus on the optimization design of distributed cooling terminals and operating strategy of the combined water loop.

Acknowledgments

This paper is supported by Project 973 (2013CB228301), National Key Technology R&D Program (2012BAA13B03) and National Science Foundation of China (51376097, 51138005).

References

[1] A.J. Shah, Exerg-Based Analysis and Optimization of Computer Thermal Management Systems, University of California Department of Mechanical Engineering, Berkeley, 2005.
[2] J.A. Olivier, J.B. Marcinichen, J.R. Thome, Two-phase cooling of datacenters: reduction in energy costs and improved efficiencies, in: 13th Brazilian Congress of Thermal Sciences and Engineering, Brazil, 2010.
[3] H.F. Hamann, A measurement-based method for improving data center energy efficiency, in: Proceedings of the IEEE International Conference on Sensor Networks, 2008.
[4] X. Wang, M. Chen, Adaptive power control for server clusters, in: IEEE International Symposium on Parallel and Distributed Processing, 2008, pp. 1–5.
[5] B. Fakhim, M. Behnia, S.W. Armfield, N. Srinarayana, Cooling solutions in an operational data centre: a case study, Appl. Therm. Eng. (2011) 2279–2291.
[6] R.K. Sharma, C.E. Bash, C.D. Patel, Dimensionless Parameters for the Evaluation of Thermal Design and Performance of Large-Scale Data Centers, Am. Inst. Aeronaut. Astronaut. (2002) 3091.
[7] J. Rambo, Y. Joshi, Thermal modeling of technology infrastructure facilities: a case study of data centers, in: W.J. Minkowycz, E.M. Sparrow, J.Y. Murthy (Eds.), The Handbook of Numerical Heat Transfer, Taylor and Francis, New York, 2005.
[8] S. Kang, R. Schmidt, K.M. Kelkar, A. Radmehr, S.V. Patankar, A methodology for the design of perforated tiles in a raised floor data center using computational flow analysis, in: Intersociety Conference on Thermal and Thermo-mechanical Phenomena in Electronic Systems, 2000.
[9] ASHRAE, Thermal Guidelines for Data Processing Environments, in: American Society of Heating, Refrigeration, and Air-conditioning Engineers, 2004.
[10] ASHRAE, Thermal guidelines for data processing environments, in: American Society of Heating, Refrigeration, and Air-conditioning Engineers, 2011.
[11] C.D. Patel, C. Bash, C. Belady, L. Stahl, D. Sullivan, Computational fluid dynamics modeling of high compute density data centers to assure system inlet air specifications, in: The Pacific Rim/ASME International Electronics Packaging Technical Conference and Exhibition, 2001.
[12] C.D. Patel, R. Sharma, C. Bash, M. Beitelmal, Thermal considerations in cooling of large scale high compute density data centers, in: Intersociety Conference on Thermal and Thermo-mechanical Phenomena in Electronic Systems, 2002, pp. 767–776.
[13] J. Rambo, Y. Joshi, Multi-scale modeling of high power density data centers, in: The Pacific Rim/ASME International Electronics Packaging Technical Conference and Exhibition, 2003.
[14] J. Rambo, Y. Joshi, Physical models in data centers airflow simulations, in: ASME International Mechanical Engineering Congress and R&D Exposition, 2003.
[15] S. Shrivastava, B. Sammakia, R. Schmidt, M. Iyengar, Comparative analysis of different data center airflow management configurations, in: The Pacific Rim/ASME International Electronics Packaging Technical Conference and Exhibition, 2005.
[16] M. Iyengar, R. Schmidt, R. Sharma, G. McVicker, S. Shrivastava, S. Shrijayantha, Y. Amemiya, H. Dang, T. Chainer, B. Sammakia, Thermal characterization of non-raised floor air cooled data centers using numerical modeling, in: The Pacific Rim/ASME International Electronics Packaging Technical Conference and Exhibition, 2005.
[17] R. Schmidt, E. Cruz, Cluster of high powered racks within a raised floor computer data center: effects of perforated tiles flow distribution on rack inlet air temperature, in: ASME International Mechanical Engineering Congress and R&D Exposition, 2003.
[18] A. Radmehr, R. Schmidt, K.C. Karki, S.V. Patankar, Distributed leakage flow in raised-floor data centers, in: The Pacific Rim/ASME International Electronics Packaging Technical Conference and Exhibition, 2005.
[19] J. Rambo, Y. Joshi, Supply air distribution from a single air handling unit in a raised floor plenum data center, in: 4th Joint Indian society of Heat and Mass Transfer – American Society of Mechanical Engineers Heat and Mass Transfer Conference, 2004.
[20] J.W. Van Gilder, R. Schmidt, Airflow uniformity through perforated tiles in a raised-floor data center, in: The Pacific Rim/ASME International Electronics Packaging Technical Conference and Exhibition, 2005.
[21] J. Niemann, J. Bean, V. Avelar, Economizer Modes of Data Center Cooling Systems, Schneider Inc White, Paris, 2011 (Paper132).
[22] Y. Chen, Y. Zhang, Q. Meng, Study of ventilation cooling technology for telecommunication base stations in Guangzhou, Energy Build. 41 (2009) 738–744.
[23] Y.T. Chang, Data center, in: Patent US8254122B2, 2012.
[24] Z. Potts, Free Cooling Technologies in Data Centre Applications, SUDLOWS White Paper, Manchester, 2011.
[25] L. Bao, J. Wang, L. Kang, The applied effect analysis of heat exchanger installed in a typical communication base station in Beijing of China, Energy Proc. 14 (2012) 620–625.
[26] J. Clidaras, D.W. Stiver, W. Hamburgen, Water-based data center, in: Patent US7525207B2, 2009.
[27] J. Choi, J. Jeon, Y. Kim, Cooling performance of a hybrid refrigeration system designed for telecommunication equipment rooms, Appl. Therm. Eng. 27 (2007) 2026–2032.
[28] A.B. Carlson, Data center cooling, in: Patent US8113010B2, 2012.
[29] W. Hamburgen, J. Clidaras, A.B. Carlson, Changing data center cooling modes, in: Patent US8295047B1, 2012.
[30] H.F. Hammann, M.K. Iyengar, T.G. Kessel, Cooling infrastructure leveraging a combination of free and solar cooling, in: Patent US8020390B2, 2011.
[31] H. Tian, Z. Li, X.H. Liu, Y. Jiang, Application study of data center heat pipe air conditioning system, Build. Sci. 26 (10) (2010) 141–145.
[32] N. Shah, CFD Analysis of Direct Evaporative Cooling Zone of Air-Side Economizer for Containerized Data Center. Ms in Mechanical Engineering, The University of Texas at Arlington, Arlington, MA, 2012.
[33] R. Tozer, C. Bash, C. Patel, Data centers, in: Patent US7903404B2, 2011.
[34] Q.H. Li, H. Huang, Z.B. Zhang, Performance experiment of heat pipe type air conditioning units for computer and data processing rooms, Heat Vent. Air Cond. 40 (4) (2010) 145–148.
[35] U. Ekstedt, M. Johansson, Heat conducting mounting structure method and radio base station housing arrangement for mounting electronic modules, in: Patent US2012/0285003A1, 2012.
[36] A. Samba, H. Louahlia-Gualous, S.L. Masson, D. Nörterhäuser, Two-phase thermosyphon loop for cooling outdoor telecommunication equipments, Appl. Therm. Eng. 50 (2013) 1351–1360.
[37] X. Jin, X.H. Qu, Z.G. Qi, J.P. Chen, Performance experiment of separate heat pipe air conditioning units for electronic equipment rooms, Heat Vent. Air Cond. 41 (9) (2011) 1336.
[38] L. Han, W. Shi, B. Wang, P. Zhang, X. Li, Development of an integrated air conditioner with thermosyphon and the application in mobile phone base station, Int. J. Refrig. 36 (2013) 58–69.
[39] A.S. Sundaram, R.V. Seeniraj, R. Velraj, An experimental investigation on passive cooling system comprising phase change material and two-phase closed thermosyphon for telecom shelters in tropical and desert regions, Energy Build. 42 (2010) 1726–1735.
[40] R. Singh, M. Mochizuki, K. Mashiko, T. Nguyen, Heat pipe based cold energy storage systems for datacenter energy conservation, Energy 36 (2011) 2802–2811.
[41] Facebook, <http://opencompute.org/servers/>.
[42] T. Brunschwiler, B. Smith, E. Ruetsche, B. Michel, Toward zero-emission data centers through direct reuse of thermal energy, IBM J. Res. Dev. 53 (476) (2009).
[43] IBM, Zurich, <http://www.zurich.ibm.com/st/energy/zeroemission.html>.
[44] Google, Commitment to Sustainable Computing, http://www.google.com/intl/qu/corporate/datacenters/step2.html, 2009.
[45] U.S. Environmental Protection Agency, Report to Congress on Server and Data Center Energy Efficiency, 2007.
[46] M. Iyengar, M. David, P. Parida, V. Kamath, et al., Server liquid cooling with chiller-less data center design to enable significant energy savings, in: 28th Annual IEEE Semiconductor Thermal Measurement and Management Symposium, 2012.
[47] R.L. Webb, N.H. Kim, Principle of Enhanced Heat Transfer, 2nd ed., Taylor & Francis, Boca Raton, 2005.
[48] X.G. Cheng, Entransy and Its Application in Heat Transfer Optimization, Tsinghua University Department of Engineering Mechanics, Beijing, 2004.
[49] Z. Li, H. Tian, H.Q. Zhang, et al., Performance optimization of separate type heatpipe heat exchanger in plant room with high density of sensible heat load, HV&AC 41 (3) (2011) 38–43.
[50] X.H. Liu, Y. Jiang, T. Zhang, et al., Match properties of heat exchange network in thermal-hygro environment building, HV&AC 41 (3) (2011) 29–37.
[51] T. Zhang, X.H. Liu, L. Zhang, Match properties of heat transfer and coupled heat and mass transfer processes in air-conditioning system, Energy Convers. Manage. (2012) 103–113.
[52] A. Ahmad, S. Rehman, L.M. Al-Hadhrami, Performance evaluation of an indirect evaporative cooler under controlled environmental conditions, Energy Build. (2013) 278–285.